THE BUNCEFIELD EXPLOSION: VAPOUR CLOUD DISPERSION AND OTHER OBSERVATIONS

J. E. S. Venart and R. J. Rogers, University of New Brunswick, Fredericton, NB, Canada

A large scale computational fluid dynamic vapour dispersion model of the release in the Buncefield incident was constructed for the western half of the accident site. The area encompassed the carparks, the Northgate, Fuji, RO and 3-Com buildings, as well as half of the first row of western storage tanks within Bund A along Buncefield Lane. Time dependent comparisons over the known period of the release of the computed $-0.1^{\circ}C$ and LFL CFD isosurfaces were made to several of the CCTV records of the developing event. The isosurface cloud extents appear to match reasonably the observed temporal and geometric developments as well as the vegetative singeing – indicative of the LFL boundary. Vehicles within the cloud, located at the cloud's western lean extremities, between the Fuji and Northgate Buildings as well as between the Northgate and 3-Com/RO Buildings, provide evidence of interior explosions prior to detonative-like crushing. Vehicles other than these appear to have been moved east by blast. Reasons for this are advanced.

Several tanks, within the tank-farm, failed by dynamic elastic crushing caused by under sudden applied radial pulse loads. These failures are also examined. In instances where the roofs were torn off some simples analysis allows estimates of the necessary internal pressures and thus required blast exposures. These results appear to confirm earlier work undertaken of the necessary external pressures to move and deform vehicles in carparks and as well as debead and deflate some of their tyres. Finite Element blast analyses applied to some of the lampposts also suggest that the blast loadings were detonative.

KEYWORDS: Blast damage, Buncefield, CFD, dispersion modelling, vapour cloud

INTRODUCTION

At about 6:00 am on Sunday December 11, 2005, the Buncefield blast occurred. There were several explosions that resulted in severe damage to the surrounding area and huge fires involving 23 fuel/oil storage tanks. A large amount of data in the form of site measurements and observations, witness statements, photographs and CCTV footage was studied and catalogued. Considerable analysis was also undertaken, most of this summarized in Steel Construction Institute, 2009, Venart and Rogers, 2010, and other papers presented in the opening session of the recent International Symposium Fire and Explosion Hazards, Leeds, April 2010.

The area covered by the vapour cloud was estimated to be around 120,000 m^2 with the average height of the cloud between 2 to 3 m. This gives a volume of between 250,000 to 375,000 m^3. Evidence suggested that the emergency pump house was one source of ignition (Steel Construction Institute, 2009).

The two most commonly known explosion mechanisms are deflagration and detonation. Both possibilities were assessed by the Buncefield Major Incident Investigation Board (MIIB) for their consistency with the observed explosion characteristics (Steel Construction Institute, 2009). Deflagration was found to be inconsistent with the significant near field damage to most objects and cars. It was also concluded to be inconsistent with the net impulse indicated by directional damage and movement to small objects, trees and posts, within the flammable cloud. Detailed CFD explosion modelling of the area immediately surrounding the emergency pump house (PH) suggested, that the trees and undergrowth along Cherry Trees Lane and Buncefield Lane could have allowed flame acceleration to several hundred m/s (J R Bakke et al., 2010, Steel Construction Institute, 2009). Such high velocity may have provided an opportunity for transition from deflagration to detonation, DDT (Deflagration-Detonation-Transition), and thus the progression of a single detonation front into the vapour cloud from the PHL (Pump-House-Lagoon) west and to the south–west.

A number of reports noted that many vehicles located in the carparks within the vapour cloud were crushed, moved, and had debeaded and deflated tyres after the explosion. Experiments and analysis by Haider et al., 2010, indicated that the minimum necessary pressure to debead and deflate tyres was about 0.8 MPa. CCTV video analyses and a simple model for vehicle sliding under the influence of detonative blast concluded (Venart and Rogers, 2010) that the statements regarding the development of the explosion up to detonation made in Steel Construction Institute, 2009, p 31; Bakke et al., 2010; and Johnson, 2010, concerning directional effects, were incorrect.

Venart and Rogers, 2010 thought the more probable development was a deflagration at the PHL that led to a large fireball, which promptly rose and dissipated. Ignition, by this source, into the surrounding uninvolved previously quiescent vapour cloud was thought to have been prevented

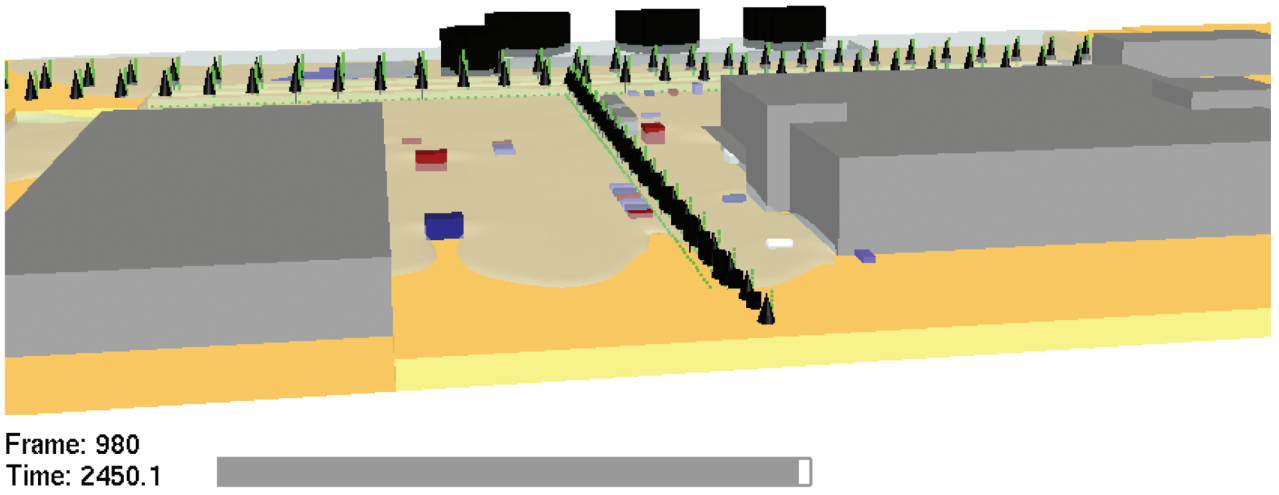

Figure 1. NIST FDS5 LES LFL dispersion model of the Buncefield release at ∼2400 s: View East between the Northgate and Fuji buildings from the Western edge of the computational domain

by the ice/water fog overlying the cold combustible mixture and seen developing on the CCTV records. Such a fog would scatter the fireball radiation upwards and attenuate any transmission downwards, as well as absorb a significant amount (Glasstone and Dolan, 1977, p 280). The fireball lift-off's positive pressure wave (its speed of sound 332 m/s; 0°C, 100% RH) could now pass through and sensitise the remaining vapour (due to its wind); causing turbulence and concentration gradients, as well as setting off vehicle alarms. These in turn to cause local vented vehicle deflagrations which were then thought to locally initiate DDT surrounding the vehicles in the cloud's now pre-sensitized lean edges[1].

Blast analyses made by Venart and Rogers, 2010, showed that most vehicle movement and crushing was caused by the positive phases of blasts originating from the west along the north and south sides of the NG building and not as envisaged by all other workers and developing from the PHL initial deflagration. Furthermore the extensive video analysis made by Venart and Rogers, 2010, clearly indicated complex multi faceted deflagrative and detonative events – not one that continuously developed.

The present paper follows up on those by Haider et al., 2010, and Venart and Rogers, 2010, to examine the vapour cloud dispersion and make qualitative/quantitative comparisons to the recently released CCTV evidence of the UK Health and Safety Executive investigation and prosecution (HSE, 2010). Photographic and video evidence of tank damage within the tank farm also allows simple analytical estimates of blast strength. Analysis of lamppost deformation and breakage, similar to that made for the movement of vehicles in Venart and Rogers, 2010, is also used to help to explain certain observed inconsistencies in lamppost behaviour.

[1]Similar to the ignition of the Port Hudson detonation (Burgess and Zabetakis, 1973); though there the pre conditioning was caused by the prevailing wind.

CFD MODEL

A NIST FDS5 (McGrattan et al., 2009) CFD model was constructed for the western half of the Buncefield site. The area modelled encompassed the carparks, the Northgate (NG), Fuji, RO and 3-Com buildings (Steel Construction Institute, 2009; Venart, 2011). The model comprised nearly two million cells ranging in size from 0.3 × 2 × 2 m to 2 × 2 × 2 m, at height, split by a mirror boundary along the N-S centreline of the line of tanks that included, in the centre, the one that overflowed; tank T912. A Schmidt Number of 1.7 and a Prandtl Number of 0.79 was taken as representative of the overflowing dispersing fuel-air cloud (Atkinson et al., 2008; Huber, 1999). In the simulation T912 overflowed ∼300 tonnes of ∼15°C wintergrade petrol for a period of nearly 40 minutes; in the process forming a 200 m diameter LFL vapour cloud.

Fence lines and vegetation (trees, fences, hedges and shrubs) were included using the version of FDS developed for use in Wildland-Urban fire interfaces (Mell et al., 2007). FDS5 uses what is called an LES turbulence model (McGrattan et al., 2009).

Figure 1 illustrates the dispersion modelling result for the lower flammable limit (LFL) boundary at about 2450 s as seen from the W based upon the reported atmospheric conditions. The LFL boundary of the simulation can be seen to conform very closely to the observed regions of vegetative singeing in the western areas between the NG, Fuji and 3-Com buildings (Steel Construction Institute, 2009).

The computed FDS5 −0.1°C, 2000–2500 s isosurfaces at the S side of water tank are nearly 8 m in height whereas the 0.046 w/w% (i.e. the LFL for the HC mixture) isosurface is at about 3.5 m – a difference of over 4 m.

And, at the fingers of the cloud that push W to embrace, the NG (Northgate) Building on both its N and S sides, the similar numbers are 6 to 7 and 1.5 to 2 m respectively. This depth of 'fog' – comprised of water droplets and possibly ice crystals – would certainly hinder and substantially reduce radiative ignition from above of any non-involved fuel outside the PHL area particularly if segregated by barriers such as berms, tree, hedge, and fence lines, as well as roadways.

Figure 2(a) shows cloud development in the space between the tanks of Bund A and the tree line of Buncefield Lane as viewed from the S at time 225 s. Figure 2(b)

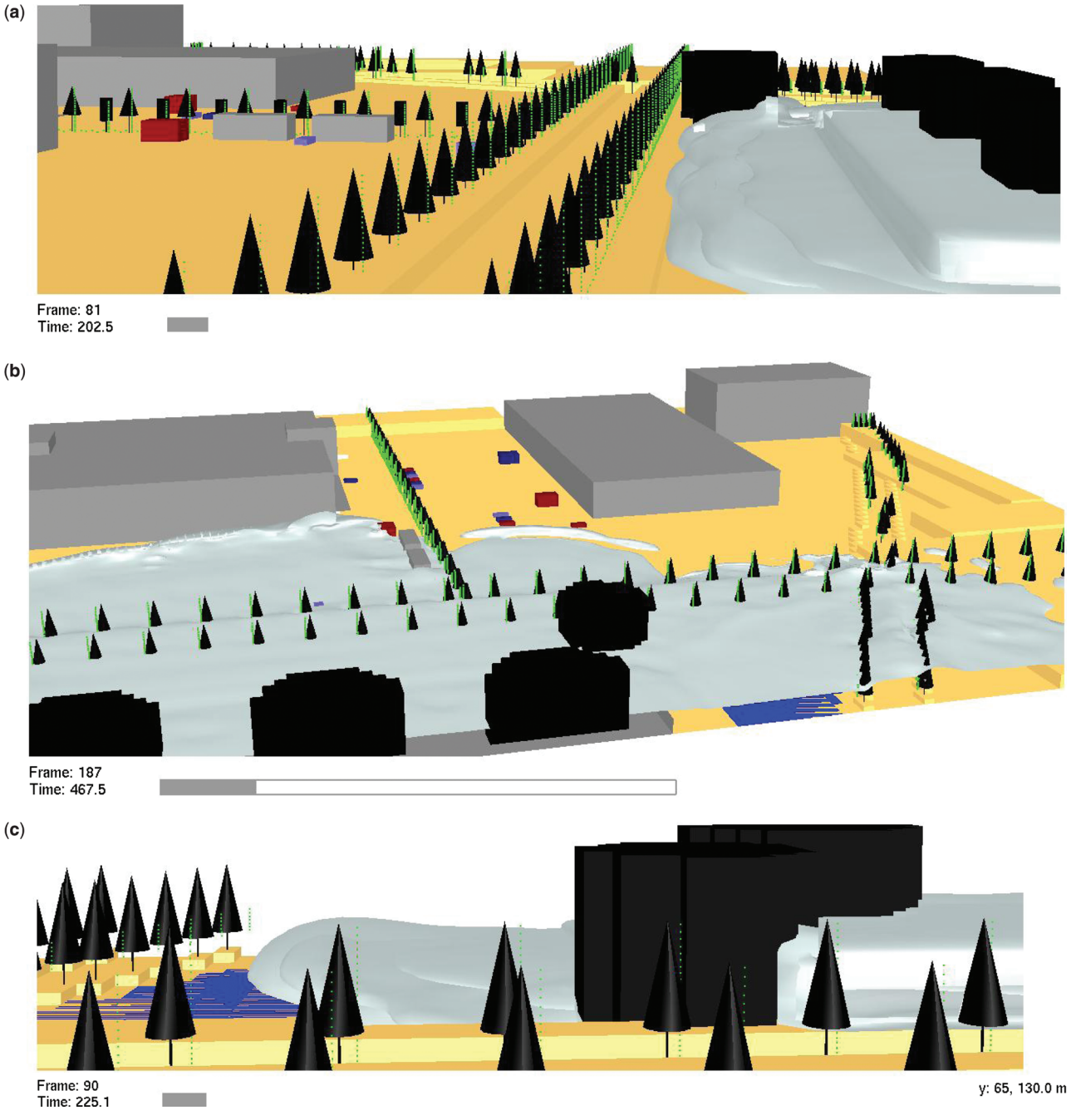

Figure 2. (a): −0.1°C vapour-cloud isosurface developing S over the space between Bund A and Buncefield Lane at 202 s; NIST FDS5 CFD simulation as viewed N towards the fire water tank. (b): −0.1°C vapour-cloud isosurface developing over the Fuji and NG carparks at about 468 s; NIST FDS5 CFD simulation as viewed towards the W from the top of the fire water tank. (c): −0.1°C isosurface developing over the PHL and around the fire water tank at 225 s as viewed from the W; NIST FDS CFD simulation

Figure 3. Aerial view to East of Bund A and its tanks. Tank T912 is in the centre foreground, T910, which was empty at the time of the incident, is to the right of T912 [*The Buncefield Incident, 11 December 2005; The final report of the Major Incident Investigation Board*, Volume 1 (2008) p 1]

illustrates the same isosurface at 467 s looking W towards the Fuji Building across its carpark. Figure 2(c) illustrates the dispersion modelling result for the -0.1°C isosurface viewed E at 202 s in the region of the PHL. All views are in reasonable temporal and geometric agreement to the CCTV evidence given in HSE, 2010, CCTV[2].

THE FAILURE OF BUNCEFIELD FUEL STORAGE TANKS T910 AND T601

There were several empty, or partially filled, large tanks within the tank farm that were damaged in a characteristic fashion – T910 (Bund A); T911, T914 (Bund B); and T6[3]. The failures consisted of the vessels being uniformly circumferentially crushed about mid-height (relative to fill level) into several lobes with plastic wrinkles; the roofs blown off – partially or completely (T910); and the roof rafters still, for the most part, attached to the outer tank circumference and exposed. For tanks of about 25 m in diameter the number of lobes or wrinkles was between 18 and 20; see Figure 3. For smaller tanks, for example, T601 to T603; the transfer storage tanks (6 m diameter and 9.8 m high), the deformations, though still crushing with lobes and wrinkles, were more numerous and complex; though all these roofs too had been torn off. Apparent reductions in volume ranged from between 55 to 60 percent for T601 and T910 respectively. This type of deformation is characteristic of what is called elastic dynamic pulse buckling and results from a suddenly applied uniform radial impulse (Lindberg and Florence, 1987). Figure 3 is the aerial overview of the tank arrangements within the bunds taken from the west.

Tanks that were full, or nearly so, such as the fire-water storage tank (W at the N end of Bund A) and T912, did not exhibit this characteristic crushing. Tank T908 and its adjacent partner to the E, both partially full and east of T912, and consequently at the southern edge of the cloud, suffered only minor elastic buckling on their northern faces and around their top circumferences where partial top tearing detachments had commenced. The fire-water storage tank appeared to be only distorted by buckling bulges around its south and eastern upper circumference walls and roof. Its walls, however, were uniformly covered by soot obviously deposited prior to any explosion[4]; the deposit on top of the tank being only partial and appearing to cover just the northern three quarter sector to the west.

Tank T910 was empty and located directly S within the same bund as T912, Figure 4. It was the same size and construction as T912 which was overflowing at the time of the incident. Its dimensions were 25 m diameter and

[2]In CCTV Evidence (HSE, 2010) it is not clear that the full extent of the video records has been provided.

[3]There were perhaps others similarly buckled (T913 and T915?) but the available photographic evidence did not permit this to be resolved.

[4]The soot deposit appears scraped/brushed off, and in some instances knocked off, by flying debris hitting the S and W tank walls. Soot deposition on the S wall of the tank appears to have been masked by the stair treads and railings.

Figure 4. Aerial view of Tank T910 from the NW. Note bottom plates peeled back along with crushed sides from the NNW. The top of the tank has been blown off the underlying rafters which then have collapsed along with the crushed walls. The apparent number of elastic lobes or wrinkles is about 20 [*Photograph provided by G Atkinson, July 2010*]

14.3 m height to the top of its shell walls. It had a conical 5 mm thick steel plate supported roof with a 1:5 pitch with a final elevation at the peak of 16.8 m from the base. A wind girder circled the wall just below the topmost 5th wall course. The roof was penetrated with eight equidistant 1 m base equilateral triangular cut-outs (total relief area $\sim$2.5 m^2) at an elevation 14.8 m based on the details given for T912. There was an open man-way ($\sim$0.6 m diameter?) near ground elevation located on the south side of the tank based upon its position on T912. Wall plate thicknesses were reported to be 10 mm for the 1st and 2nd courses; 8 mm, the 3rd and 4th; and 6 mm the 5th to 8th courses (Atkinson, 2010). Weld sizes were assumed the minimum specified by API 620 E10 (2004) for the given diameter; 6.35 mm and 5 mm respectively. Tank T910 would have contained about 7440 m^3 or 9680 kg of air.

In Figure 4 tank T910 is shown crushed and its plate roof torn and blown off – a piece of the roof was found in the Northgate carpark and another was just immediately over Bund A to the east. Blast impact appears to have been from the NNW with significant peeling of its base plate as well as tearing of the wall/base junction to the south[5]. Over much of the NNW side wall deformation appears to consist of many, nearly identical, lobes wherein there are significant regions of crushing followed by reverse bending/bulging and, in these locations, localized regions of plate tearing. The shell walls to the SSW appear to have been torn away from their base plate and the roof. The roof structural steel rafters appear to have collapsed along with the top shell walls.

Tanks T6, T911 and T914 appear similarly crushed with roofs either blown off or partially detached (Figure 3).

At the time of the explosion the empty portions of the tanks would have been full or partially full of air/product vapour or the vapour cloud; entering in the case of T910 through its open base man-way. If, as suspected, the tanks had been hit by a Butane vapour-cloud detonative blast, its CJ blast wave transit time would have been about 14 ms front to back; $\sim$1800 m/s. Considering the duration of a linearized positive phase dynamic overpressure pulse to be about 5.4 ms (HSE rr718, Appendix H, Fig. H8 p 164) and the structure's characteristic elastic response time of the order of 300 ms (Lindberg and Florence, 1987, p 188) it must be concluded that the loading was impulsive and that the blast would have resulted in significant fluid/structure interaction (FSI); i.e. there would have been immediate elastic collapse of the walls and any negative pressure drag loading of no consequence to the structure's further response.

As the structure collapsed internal shocks will have been produced in the trapped gases and the internal gas compressed. It is worthwhile to speculate how this might have happened, Figure 5.

The maximum amount of energy that can be deposited by a detonative wave in the volume occupied by the tank can be estimated based upon ideal blast wave theory. First the maximum positive over-pressure is known to be 1.9 MPa if CJ for Butane and this value rapidly falls to ambient over a period of some 5.4 ms (assuming a linear variation of pressure with time). Thus the average energy per unit volume of the wave is about 0.95 MPa and the

[5]How much of this is due to blast wave reflection and amplification south from T912 is uncertain though work by Oakley et al. 2001 indicates significant ($\sim$35%) increases in the forces experienced by the following cylinder in a three cylinder triangular array. This is attributed to decreasing flow area.

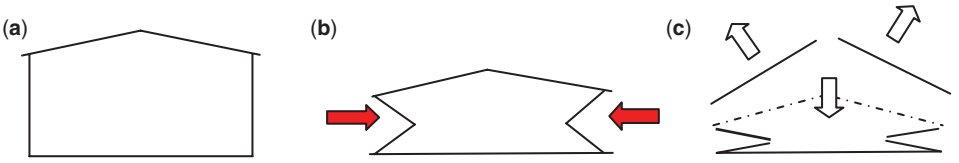

Figure 5. Crushing interaction of a positive blast shock front with an empty, or partially empty, roofed cylinder; e.g. T6, T910, T911, T914. Before: (a) Blast crushing: (b) Roof being blown off, walls and rafters collapsing: (c)

impulse some 5 kPa-s. If the thickness of the combustible portion of the vapour cloud around the tanks is assumed to be 4 m (based upon the berm height and CFD studies) this means that within a volume equal to that of the tank to the height of the vapour cloud (1963 m^3) 1865 MJ of energy could have been deposited; i.e., in the time it takes the wave to transit the tank the available power is about 130 GW.

We know that the roof of T910 was torn off the tank edge and its radial rafters and transverse purlins. A lower bound of the internal pressure necessary to do this can be estimated. Based upon a tensile shock loading factor of say 1.3; a flow stress ((yield + ultimate)/2) for mild steel, ~280 MPa; and a plate/weld thickness of 5 to 6 mm with the area of the roof $\pi/2 \times 25 \times 12.74 = 500\ m^2$; and knowing that the roof of T910 was torn from the necessary sealing welds to tank walls, as well as in half, the minimum internal pressure, P_{int}, can be estimated. This is $(\pi \times 25 + 25) \times 0.005 \times 1.3 \times 280/500$ or $P_{int} = 0.38$ MPa.

Assuming the compression process is isentropic, and there is no escape or entry from or to the contained air due to chokes, the change in air volume can be evaluated along with the work necessary for its compression. To this we will have to include the necessary crushing, bulging, peeling, and tearing work of the metal.

Thus we have $PV^{\gamma} = \text{constant}$ and the crushed volume at the instant of top detachment 2879 m^3; or a reduction in volume of some 60%. The compression work on the gas necessary to achieve this is 9680 kg × 0.714 kJ/kgK (127 K) or 895 MJ.

The energy content of a combustible cloud, if Butane (HHV 45.4 MJ/kg) at 6 w/w% 4 m deep (CFD study), would be associated within a 5 m wide annular volume surrounding the tank (~35 m diameter, 4 m deep) if the combustion efficiency was say 95%. The fact that the detonative wave did not enter the tank via the open man-way, located nearly opposite the point of blast impact, confirms that the original blast must have been a detonation since the tank did not explode and the man-way opening was of the order of 10 detonative cell widths (0.054 m).

The crushing of the transfer tanks T601 to T603 (6.0 m D × 9.8 m H) was much more complex than that for tank T910. Figure 6(a) is an aerial view of the tanks from the west and Figure 6(b) a view looking to the north–west. All tanks have had their membrane top roofs torn and blown off. The tanks were obviously only partly full at the time. Apparent reductions in volumes, based on the observed liquid level and deformation of the most northern tank, appear to be about 55 percent. Blast transit times, based upon an assumed CJ Butane detonation, would have been about 3 ms with elastic characteristic time of about 90 ms based upon an assumed wall thickness of 5 mm (assumed weld thickness 3.5 mm). Analysis, similar to that for T910, yields a minimum crushing pressure to tear off these roofs as 0.85 MPa.

It can be concluded therefore that tanks T910 and T601 were crushed by elastic impulse pulse buckling with blast loading overpressures of between 0.38 and 0.85 MPa. The last of these values compare favourably with that

Figure 6. (a) Transfer tanks T601 to 603 as seen from the SW; (b) T601 to T603 as seen from the NE. These tanks are 6 m in diameter and 9.8 m tall. The tanks were obviously partially full at the time of crushing (Atkinson, 2010)

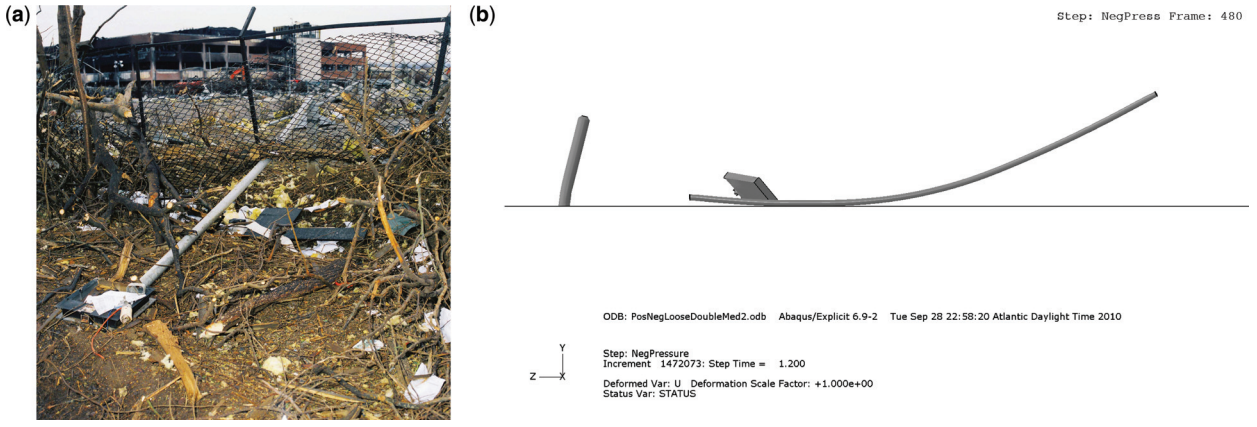

Figure 7. Fuji carpark lampposts: (a) Lamppost in foreground has been hit by blast, snapped and then felled NE. The Fuji carpark Buncefield perimeter fence has next been blown down, up over the felled lamppost base, and then dragged over the fallen pole. A similar pole in the background has also been snapped and blown down to the E. (b) Abaqus/Explicit 6.9 FE simulation of a similar lamppost indicating the fracture at base, removal of lamp housing, and displacement, all in the direction of the blast's positive phase.

required to debead and deflate the vehicle tyres noted in the carparks, i.e. 0.8 MPa (Haider et al., 2010), and the mean average blast over-pressure of a Butane CJ detonation, 0.95 MPa[6].

LAMPPOST BLAST LOADING AND DEFORMATION

Venart and Rogers, 2010, in their analyses of CCTV records from the RO and Furnel Buildings noted that the Buncefield event was very complex consisting of two major deflagrative and two, near simultaneous, detonative events. The Steel Construction Institute's HSE report rr718 and others, however, concluded that the explosion resulted from flame acceleration up Three Cherry Tree Lane to DDT and then W into the Fuji and NG carparks and down Buncefield Lane; i.e., a continuously developing event. Directional evidence in the form the deformation and snapping off of lampposts, fence posts, CCTV masts, trees, etc. and assumed representative of the negative phase pressure loading was used in support of this conclusion. There were, however, several inconsistencies in the observed data for the lampposts. In particular most lampposts in the carpark to the E of the NG Building appeared to be vertical and not deformed – though many had been abraded by dust and grit on particular sides at their bases. This observation, based upon the assumption that the abrasion was the result of a negative pressure phase of the explosion, was used to infer blast direction. On the other hand lampposts, fence posts, and other indicators (e.g. trees) at the S edge of the Fuji carpark were badly deformed, bent and some collapsed or snapped/fractured most pointing E or NE – some confusingly so.

For example Figure 7(a) shows a fractured lamppost felled to the NE (with another to the W behind it felled to the E). Here the perimeter fence between the Fuji carpark and Buncefield Lane appears blown overtop of the already felled lamppost. In an attempt to understand this and other behaviour, several lamppost FE (Finite Element) models were constructed and subjected to blast loadings using the ideal blast model taken from Venart and Rogers, 2010. The Abaqus/Explicit FE code v6.9.2 (2009) was used in these simulations.

It was hypothesized that a lamppost might have experienced two opposite load steps due to over-pressure events. The first and positive load step acting toward the east was taken as 5.4 ms (Venart and Rogers, 2010). This over pressure was assumed to decrease linearly with time. The pressure acting on the lamppost components during this load step is the dynamic pressure q given by $5/2\ p^2/(7p_0 + p)$ where p is the time dependent blast pressure decreasing from 1.8 MPa behind the shock front with p_o atmospheric pressure; the density ρ behind the shock front given by $\rho_o[(7 + 6p/p_0)/(7 + p/p_0)]$; with the corresponding particle, or wind, velocity V given as $(5p/7p_0) \cdot c_0/(1 + 6p/7p_0)^{\frac{1}{2}}$, with c_0 the ambient speed of sound (ahead of the shock front). All properties are determined based upon the Rankine-Hugoniot conditions for a true (or ideal) shock wave, Glasstone and Dolan, 1977.

The second load step considered an air velocity of 300 m/s in the opposite direction. The first ramp was taken as linear over 20 ms, constant for 120 ms and then linear to zero in 20 ms (Steel Construction Institute, 2009). The drag pressure on the lamppost is given by $-\frac{1}{2}C_D\rho_o V^2$ where $C_D = 1$. The negative drag pressure acts on the projected area of the post in a constant westerly direction. The relative velocity of the lamppost is neglected; since the peak lamppost velocity is approximately 60 m/s; this is not a major simplification. Following these two load steps would be a period of free movement until the post and its components come to rest.

The lamppost analyzed was similar to the one shown in Figure 7(a). Its assumed components (length units

[6]Vasil'ev, 2009 gives the detonation pressure for Butane as 1.84 MPa.

converted to m in the model) consisted of (a) main pole: 24 ft. long 3 in. schedule 40 steel pipe (O.D. 3.5 in. and thickness 0.216 in.), (b) base: 4 ft. long 6 in. schedule 40 steel pipe (O.D. 6.25 in. and thickness 0.28 in.), (c) connecting cone: slope 45 degrees, 0.28 in. thick, (d) connecting flange inside base: at 24 in. from bottom, between base pipe and main pole, 0.28 in. thick, and (e) top box: 18 in. by 36 in by 4 in. high, steel 0.0625 in. thick, holes on top and bottom surfaces to fit the main pole.

The material was taken as steel (Dyapole, 2004; Schmidt et al., 1989) with a yield strength of 345 MPa (50 ksi) and used the following plastic strain/stress (MPa) hardening values: 0, 345; 0.01, 375; 0.03, 400; 0.05, 410. The ductile damage initiation was taken as: fracture strain (PEEQ) = 0.2; triaxial stress (TRIAX) = 0.6; strain rate (ER) = 20; with local displacement at failure: 1.5 mm. No damping was considered except for material plastic behaviour and friction.

The mesh consisted of 5338 linear shell elements with reduced integration, 32514 degrees of freedom; with 36 elements around the circumference of the pipes and a graduated length-wise mesh in the pole near top of the base and below the lamp box. All joints were "*tied*" except between lamp box and pole where a friction interaction was chosen. The boundary conditions were fully fixed at the bottom with a rigid analytical surface for friction contact with ground; friction coefficient = 0.4.

The loading consisted of the gravity load applied gradually for 0.05 s with damping to avoid numerical waves; the pressure load (general traction along a horizontal direction) on the pipe surface and box end nearest pipe (the pipe surface load was scaled equivalent to its projected area). The positive load peak was 3.24 MPa decreasing to 0 in 5 ms; the negative load peak was 57.2 kPa.

The solution was obtained using a central time difference algorithm, nonlinear geometry, double precision, a time step of 0.5 to 0.8 μs, with output every 1 ms in the positive pressure load phase and every 2.5 ms for the negative pressure load phase. A solution duration of 1.2 s for the negative pressure load phase gave a total simulation time of 1.255 s; this required a clock-time of about 15 hrs on 2 parallel processors in a 1.33 GHz laptop computer.

Figure 7(b) shows the final configuration of a lamppost simulation where its total length was exposed to blast. The simulated system is not quite at rest and further vertical settling will occur. The base post shows a permanent lean in the direction of the positive pressure. The pole snapped at the base-pole connection and lamp box landed to the east of the base post, consistent with the actual lampposts shown in Figure 7(a). The simulated lamp box separated at 0.063 s of pressure loading and landed rather close to the base post, whereas the lamp box in Figure 7(a) is near the far end of the pole.

The fence and debris overriding the felled post in Figure 7(a) suggests that after being felled by blast, debris was blown into the fence and then this collection was deposited overtop. This suggests strongly that the blast was followed by a powerful deflagrative event.

CONCLUSIONS

A large scale eddy simulation computational fluid dynamic model of the dispersion of the petrol vapour release in the Buncefield incident was constructed for the western half of the accident site. The computed isosurfaces of temperature and concentration are in reasonable temporal and geometric agreement to the CCTV record given in HSE evidence. The computational data can be utilized to estimate the distribution and cloud thickness, composition and temperature over time and thus its potential flammable and explosive content. A more refined and extensive dispersion model is to be desired that would include more of the tank farm. A CFD explosion model of the tank farm would also be useful in assessing blast direction which appears to the present authors to be predominantly west to east consistent with the overall damage pattern in the tank farm, vehicles in the carparks, and with the lampposts.

Tanks T910 and T601 were crushed elastically by an impulse pressure pulse that resulted in their buckling and tearing off of their roofs. Minimum blast overpressures of between 0.38 and 0.85 MPa are required to do this. The 0.85 MPa value compares favourably with that required to debead and deflate the vehicle tyres noted in the carparks and the mean average blast over-pressure of a Butane CJ detonation. Finite element models of these tanks in response to blast are desirable to confirm this.

Most lampposts in the carpark to the east of the NG Building appeared to be *vertical* and *not* deformed and thus have *not* been exposed to large positive pressure pulses. On the other hand lampposts, fence posts, and other indicators (e.g., trees) at the S edge of the Fuji carpark were badly deformed, bent and some collapsed or snapped/fractured most pointing E or NE. Simulations of the response of a lamppost to positive and negative phase pressure pulses (consistent with the in-vehicle detonation initiation hypothesis) also fractured off and landed east of its base post. The observed overriding of the blast felled pole by the fence and its collected debris suggests that after blast there was a powerful deflagrative event.

REFERENCES

Abaqus Analysis User's Manual v6.9, 2009, Online Documentation, Dassault Systemes Simulia Corp., Providence, RI, USA.

API Standard 620, 2004, "Design and Construction of Large Welded, Low Pressure Storage Tanks," Tenth Edition, February 2002, Addendum 1, June 2004, American Petroleum Institute, Washington, DC.

Atkinson, G., 2010, private communication.

Atkinson, G., Grant, S., Painter, D., Shirvill, L., and Ungut, A., 2008, "Liquid Dispersal and Vapour production During Overfilling Incidents." I Chem E Symp Series No 154.

Bakke, J.R., van Wingerden, K., Hoorelbeke, P., and Brewerton, R., 2010, "A study on the effect of trees on gas explosions," *J Loss Prevention in the Process Industries*, doi: 10.1016/j.jlp.2010.08.007.

Burgess, D.S. and Zabetakis, M.G., 1973, "Detonation of a Flammable Cloud Following a Propane Pipeline Break; The December 9, 1970, Explosion in Port Hudson, Mo.," United States Department of the Interior, Bureau of Mines, Report of Investigation 7752, Washington, DC, 26 p.

Dynapole, TRS series, tech. details, 2004, http://www.dynapole.com/gifs/products/trs.pdf

Glasstone, S. and Dolan, P.J., 1977, "The Effects of Nuclear Weapons," United States Department of Defense and the Energy Research and Development Administration, Washington, DC.

Haider, M.F., Rogers, R.J., and Venart, J.E.S., 2010, in press, "External pressures required to debead tyres," *Proceedings ISFEH6, Leeds, April.*

HSE, 2010, Buncefield Evidence, UK Health and Safety Executive Website, July 2010.

Huber, M.L., 1999, NIST Standard Reference Database 4, THERMOPHYSICAL PROPERTIES OF HYDROCARBON MIXTURES, SUPERTRAPP, Ver 3.00, National Institute of Standards and Technology, Gaithersburg, MD.

Lindberg, H.E. and Florence, A.L., 1987, "Dynamic Pulse Buckling", Martinus Nijhoff, Dordrecht.

Johnson, D.M., "The potential for vapour cloud explosions – Lessons from the Buncefield accident", 2010, *Journal of Loss Prevention in the Process Industries*, doi: 10.1016/j.jlp.2010.06.011.

McGrattan, K., Hostikka, S., Floyd, J., Baum, H., Rehm, R., Mell, W., and McDermott, R., 2009, "Fire Dynamics Simulator (FDS) ver. 5, Technical Reference Guide", National Institute of Standards and Technology, Gaithersburg, MD.

Mell, W., Jenkins, M.A., Gould, J., and Cheney, P., 2007, "A physics-based approach to modeling grassland fires", *Int. J. Wildland Fire* **16**: 1–22.

Oakley, J.G., Anderson, M.H., Wang, S., and Bonazza, R., "Shock Loading of a Cylinder Bank with Imaging and Pressure Measurements," 2001, 23rd Int. Symp. Shock Waves, Fort Worth TX, 22–27 July.

Schmidt, L.C., Lu, J.P., and Morgan, P.R., 1989, "The influence on steel tubular strut load capacity of strain hardening, strain aging and Bauschinger effect," *Journal Construction Steel Research* **14**: 107–119.

Steel Construction Institute, 2009, "Buncefield Explosion Mechanism; Phase 1," Volumes 1 and 2, Health and Safety Executive (HSE), rr718, December, 226 p.

"The Buncefield Incident 11 December 2005: The Final Report of the Major Incident Investigation Board": **1**, Fig. 5, p 8 (2008).

Vasil'ev, A.A., 2009, "Detonation Properties of Saturated Hydrocarbons," *Combustion, Explosion, and Shock Waves* **45**: 6, pp. 708–715.

Venart, J.E.S., 2011, in preparation.

Venart, J.E.S. and Rogers, R.J., 2010, in press, "Buncefield: Questions on the Development, Progression, and Severity of the Explosion," *Proceedings ISFEH6, Leeds, April*.